Lamellar Morphology of Poly(trimethylene terephthalate)/ Poly(ether imide) Blends Studied via Small-Angle X-ray Scattering

Hsiu-Jung Chiu,[1] Jieh-Ming Huang[2]

[1]*Department of Chemical and Materials Engineering, Ta Hwa Institute of Technology, Hsinchu, 30703, Taiwan, Republic of China*
[2]*Department of Chemical and Materials Engineering, Van Nung University, Chung-Li, 30703, Taiwan, Republic of China*

Received 21 March 2005; accepted 9 May 2005
Published online 16 December 2005 in Wiley InterScience (www.interscience.wiley.com).
DOI 10.1002/app.22219

ABSTRACT: The lamellar morphology of a melt-miscible blend consisting of poly(trimethylene terephthalate) (PTT) and poly(ether imide) (PEI) prepared by solution precipitation has been investigated by means of optical polarized microscopy (POM) and small angle X-ray scattering (SAXS). From the observation under POM, it was suggested that PEI was predominantly segregated into the interlamellar and/or interfibrillar regions upon PTT crystallization since the PTT spherulitic morphologies of blends were volume-filling. From results of SAXS data analysis, a larger amorphous layer thickness was identified in the blends, showing that some PEI was incorporated inside the interlamellar regions after crystallization. Despite the swelling of the amorphous layer, the amorphous layer thickness was relatively independent of the blend composition. It was concluded that amorphous PEI was located in the interlamellar regions of PTT as the weight fraction of PEI (w_{PEI}) [$\leq$] 0.1, while amorphous PEI was predominantly segregated into the interfibrillar regions of PTT as $w_{PEI} > 0.1$, and the extent of interfibrillar segregation increased with increasing w_{PEI}.
 J Appl Polym Sci 99: 2421–2427, 2006

Key words: segregation morphology; poly(trimethylene terephthalate); poly(ether imide); interfibrillar segregation

INTRODUCTION

Poly(trimethylene terephthalate) (PTT) is a linear aromatic polyester with three methylene moieties in the repeating unit. Although chemical structures are similar to poly(ethylene terephthalate) (PET) and poly(butylenes terephthalate) (PBT), the physical properties of PTT are much different from those of PET and PBT. PTT with excellent and economical properties for the applications such as films and fiber has been developed by Shell Chemical Company.[1–5] However, a lower glass transition temperature (T_g = 44°C) of PTT is a disadvantage in some applications. Since PTT is a crystalline polymer, its physical properties are expected to depend strongly on its crystalline morphology, which can be controlled by the crystallization kinetics. Blending the PTT with other polymers is an effective way for tuning the crystalline morphology. Poly(ether imide) (PEI) is a high-performance engineering plastic with a very high T_g (~215°C).[6] PEI also possesses several advantageous properties such as excellent toughness and good electrical insulation, while PEI has a poor chemical resistance due to its amorphous nature. Therefore, it is expected that blending of PTT and PEI will offer an interesting route to combine the complementary properties of both polymers. Huang et al.[6] found that the PTT/PEI blends were miscible in the melt for the entire composition since the blends showed a single and composition-dependent T_g over the entire composition range and the crystallization kinetics also decreased with the addition of PEI. In the present study, we are interested in the investigation on the microstructure morphology of the PTT/PEI blends since the bulk physical properties are also stemmed from the microstructure morphology.

For a crystalline/amorphous system, the crystallization usually involves two types of polymer transport: diffusion of the crystalline component toward the crystal growth front and simultaneous segregation of the amorphous diluent away from the growth front. The diluent segregation can take place on three length scales, namely, interlamellar, interfibrillar, or interspherulitic. Interlamellar segregation occurs when the diluent is incorporated into the amorphous regions between individual lamellae. Interfibrillar segregation is characterized by the segregation of the amorphous diluent to the regions between the lamellar stacks,

Correspondence to: H.-J. Chiu (hjc@thit.edu.tw).
Contract grant sponsor: National Science Council; Contract grant number: NSC 93–2216-E-233–002.

which consequently generates amorphous domains in between the lamellar stacks. Interspherulitic segregation is associated with the longest segregation distance, where the diluent is expelled out of the spherulites. Different morphological patterns may coexist in a given blend, leading to multiple locations for the amorphous diluent. These morphological patterns represent the diluent dispersion from the nanoscopic scale to the micrometer scale. Different scales of dispersion may lead to different properties.

In this article, we will investigate the microstructure morphologies of the PTT/PEI blends by means of small-angle X-ray scattering (SAXS). The effects of composition and thermal history on the segregation morphology of crystalline/amorphous state in the PTT/PEI blends will be discussed via SAXS data.

EXPERIMENTAL

Materials and sample preparation

PTT with $M_n = 2.1 \times 10^4$ and $M_w = 4.63 \times 10^4$ was obtained from Shinkong Synthetic Fibers Co. Taiwan. PEI with $M_w = 1.2 \times 10^4$ and $M_w = 3.0 \times 10^4$ was acquired from General Electrical (GE, Ultem 1000) Co. America. PTT were blended with PEI by solution precipitation. A series of PTT/PEI blends of designated weight composition ratios were stirred and dissolved in dichloroacetic acid at 80°C. These blends were subsequently recovered by precipitation in 10-fold excess volume of water. The blends were thoroughly washed with a large amount of water and then dried in a vacuum oven at 105°C for 3 days.

Samples for SAXS study were prepared by pressing the blends between two pieces of Teflon films on a Linkam HFS91 hot stage at 270 ± 0.2°C for 3 min. The samples were subsequently transferred directly into an oven equilibrated at the desired crystallization temperature (T_c) to allow the crystallization of PTT for 5 h. Optical microscopy confirmed that volume-filling spherulitic samples were obtained through such a crystallization condition.

Polarized optical microscopy

The spherulitic morphology and growth were monitored with a Zeiss polarized optical microscope. The sample was first melted on a Linkam HFS91 hot stage at 270 ± 0.2°C for 3 min, and then quickly transferred to another hot stage equilibrated at the desired crystallization temperature (T_c), where the spherulitic growth was monitored. Micrographs were taken at intervals for measuring the spherulite radii (R) at various time periods. The growth rate was calculated from the change of spherulitic radius with time, dR/dt.

SAXS measurement

The SAXS experiments were conducted at the Department of Chemical Engineering, National Tsing Hua University, Taiwan. SAXS measurements were performed using a Bruker NanoSTAR SAXS instrument. The X-ray source, a 1.5 kW X-ray generator (Kristalloflex 760) equipped with a Cu tube, was operated at 35 mA and 40 kV. The scattering intensity was detected by a two-dimensional position-sensitive detector (Bruker AXS) with 512 × 512 channels. All data were corrected by the empty beam scattering, the sensitivity of each pixel of the area detector. The area scattering pattern has been radially averaged to increase the photon counting efficiency compared with the one-dimensional linear detector. The intensity profile was output as the plot of the scattering intensity (I) versus the scattering vector, $q = 4\pi/\lambda \sin(\theta/2)$, where θ is the scattering angle and λ is the X-ray wavelength.

Bulk crystallinity measurements

Bulk crystallinities of crystallized PTT/PEI blends were calculated from the enthalpy of melting (Δh_f). The sample used for Δh_f measurement was cut directly from the specimens for SAXS measurement. The enthalpy of melting was measured by a METTLER TOLEDO DSC822e differential scanning calorimeter (DSC). The bulk crystallinity (ϕ_c) was calculated by taking 146 J/g as the enthalpy of melting of 100% crystalline PTT,[3,7] i.e., $\phi_c = \Delta h_f / 146$.

RESULTS AND DISCUSSION

Spherulitic morphology

The spherulitic morphology of crystalline polymers can be readily observed by POM. Figure 1 shows the spherulitic morphologies of PTT/PEI blends crystallized at T_c = 190°C. PTT spherulitic growths were observed to be linear with time and no apparent evidence of liquid–liquid phase separation was found up to the point of spherulite impingement for blend compositions studied. The observed spherulitic morphology was volume-filling, implying that the PTT/PEI blends mainly created the intraspherulitic segregation (i.e., interlamellar or interfibrillar segregation).

Lamellar morphology

The lamellar microstructure of a crystalline/amorphous polymer blend can conveniently be probed from the profile of scattering intensity ($I(q)$) with scattering vector (q) through the SAXS measurement. In the present study, we utilized the SAXS technique to probe the lamellar morphologies of PTT/PEI blends. Figure 2 depicts the Lorentz-corrected SAXS profiles of PTT/PEI blends crystallized at T_c = 200, 180, 160°C,

respectively. In Figure 2, we observed the scattering peak (q_{max}) associated with the electron density contrast between the alternating crystalline and amorphous layers at each blend composition. The q_{max} shifted to a smaller position with the addition of 10 wt % PEI content and then maintained seemingly unchanged with further increasing PEI composition, indicating the value of long period (L^{Bragg}) calculated by Bragg's law ($L^{Bragg} = 2\pi/q_{max}$) for blends at each T_c is remained constant but its value is larger than that of neat PTT.

The morphological parameters including the crystal thickness (l_c), amorphous layer thickness (l_a), and the long period ($L = l_c + l_a$) may be evaluated by the one-dimensional correlation function ($\gamma(z)$)[8] defined to:

$$\gamma(z) = \frac{1}{Q}\int_0^\infty q^2 I(q)\cos(qz)\, dq \quad (1)$$

where z is the direction along which the electron density is measured. Q is the scattering invariant.

$$Q = \int_0^\infty I(q)q^2\, dq \quad (2)$$

Since the experimentally accessible q range is finite, extrapolation of intensity to both low and high q is necessary for the integrations. Extrapolation to zero was accomplished by the Debye–Bueche model[9]

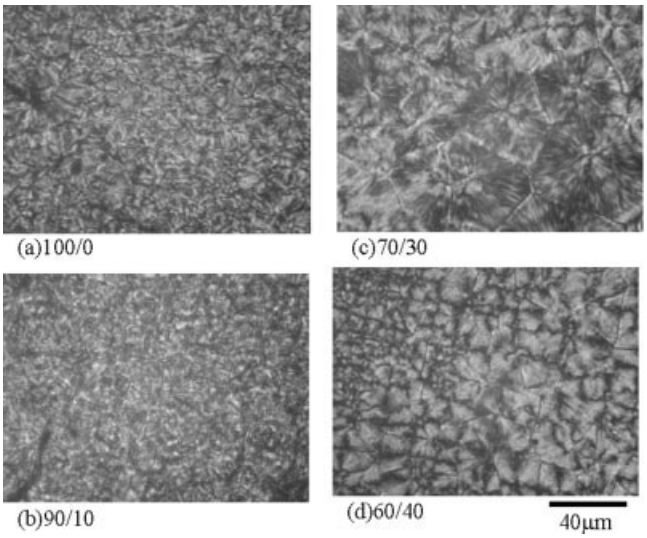

Figure 1 Spherulitic morphologies of PTT/PEI blends crystallized at T_c = 190°C under POM.

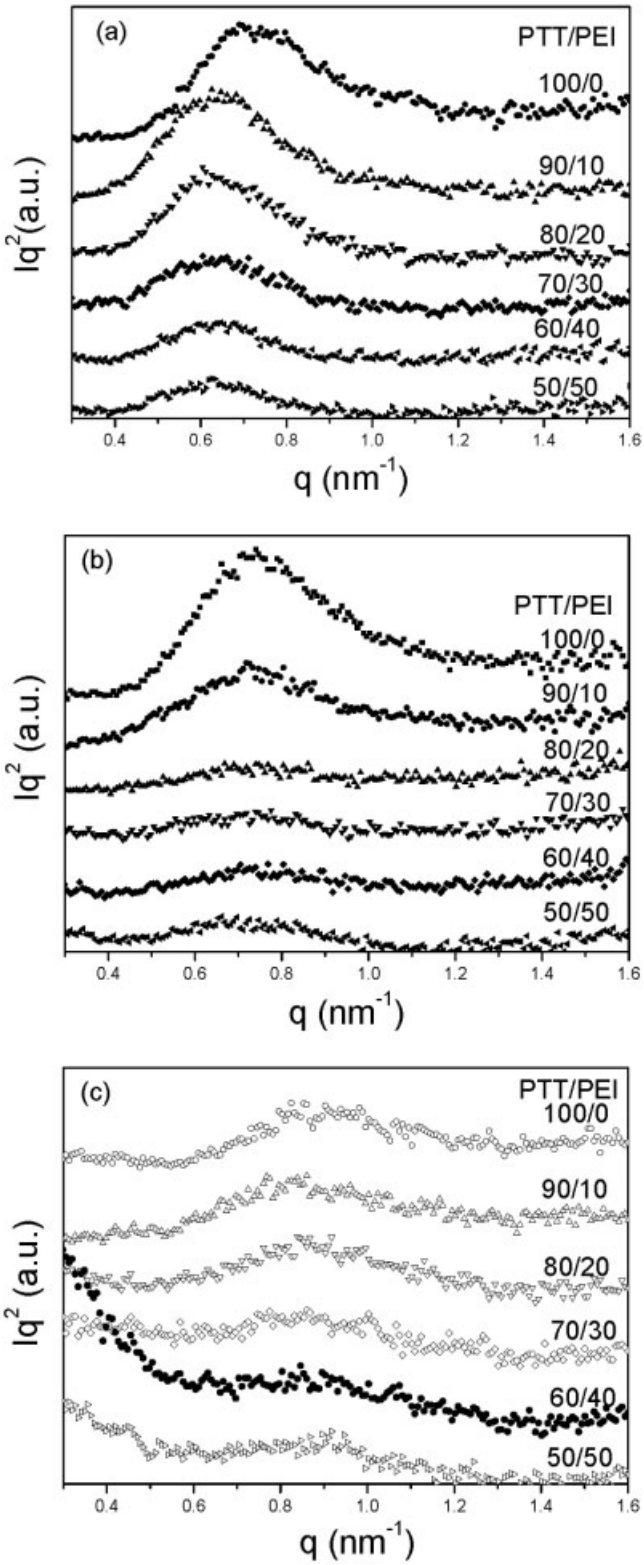

Figure 2 Lorentz-corrected SAXS profiles of PTT/PEI blends crystallized at (a)T_c = 200°C; (b) T_c = 180°C; (c) T_c = 160°C.

$$I(q) = \frac{A}{(1 + a_c^2 q^2)^2} \quad (3)$$

where A is a constant and a_c is the correlation length. A and a_c can be determined from the plot of $I(q)^{-0.5}$ versus q^2 using the intensity data at low q region. Extension to large q can be performed using the Porod–Ruland model[10–11]

$$I(q) = K_p \frac{\exp(-\sigma^2 q^2)}{q^4} + I_{fl} \quad (4)$$

where K_p is the Porod constant, σ is a parameter related to the thickness of interphase between crystal and amorphous layers, and I_{fl} is the background intensity arising from thermal density fluctuation. The values K_p, σ, and I_{fl} were obtained by curve fitting the intensity profile at high q region. Figure 3 shows the one-dimensional correlation functions of PTT/PEI blends crystallized at various T_cs. Assuming the corresponding two-phase model, l_c, l_a, the most probable value of L can be estimated via simple geometric analysis of $\gamma(z)$, as demonstrated in Figure 4. The thickness of the thinner layers (l_1) is given by the intersection between the straight line extended from the self-correlation triangle and the baseline given by –A[8]. The average thickness of the thicker layer is then obtained from $l_2 = L - l_1$. The assignment of l_1 and l_2 is governed by the magnitude of the linear crystallinity (ϕ_c^{lin}). When $\phi_c^{lin} < 0.5$, the crystals contribute the smaller thickness; then $l_1 = l_c$ and $l_2 = l_a$. The inverse is true for $\phi_c^{lin} > 0.5$. Linear crystallinity, ϕ_c^{lin} is defined as

$$\phi_c^{lin} = \frac{l_c}{L} = \frac{l_c}{l_c + l_a} \quad (5)$$

Provided that spherulites are volume-filling, ϕ_c^{lin} is related the bulk crystallinity, ϕ_c by

$$\phi_c = \phi_s \phi_c^{lin} \quad (6)$$

where $\phi_s = \phi_c/\phi_c^{lin}$, the volume fraction of lamellar stacks in the sample. Since $\phi_s < 1$, eq. (6) prescribes that the bulk crystallinity cannot be higher than the linear crystallinity. As a result, the assignment of l_1 and l_2 would be rather straightforward if the bulk crystallinity is greater than 0.5, because in this case the larger length, l_2, must correspond to the crystal thickness and l_1 to the amorphous layer thickness. In the present study, for neat PTT and all blend compositions at each T_c, ϕ_c is below 0.5 as shown in Figure 6, it is reasonable to assign $l_1 = l_c$ and $l_2 = l_a$.

Figure 5 shows the variations of L, l_c and l_a with the weight fraction of PEI (w_{PEI}) at various T_cs. It is observed in Figure 5(a) that the L value increased as the addition of 10 wt % PEI content but did not vary with further increasing PEI content. This result is consistent with the observation in Figure 2. From the observation in Figure 5(b), it is obvious that the l_c value increased with elevating T_c. According to the secondary nucleation theory,[12–13] the initial crystal thickness is given by

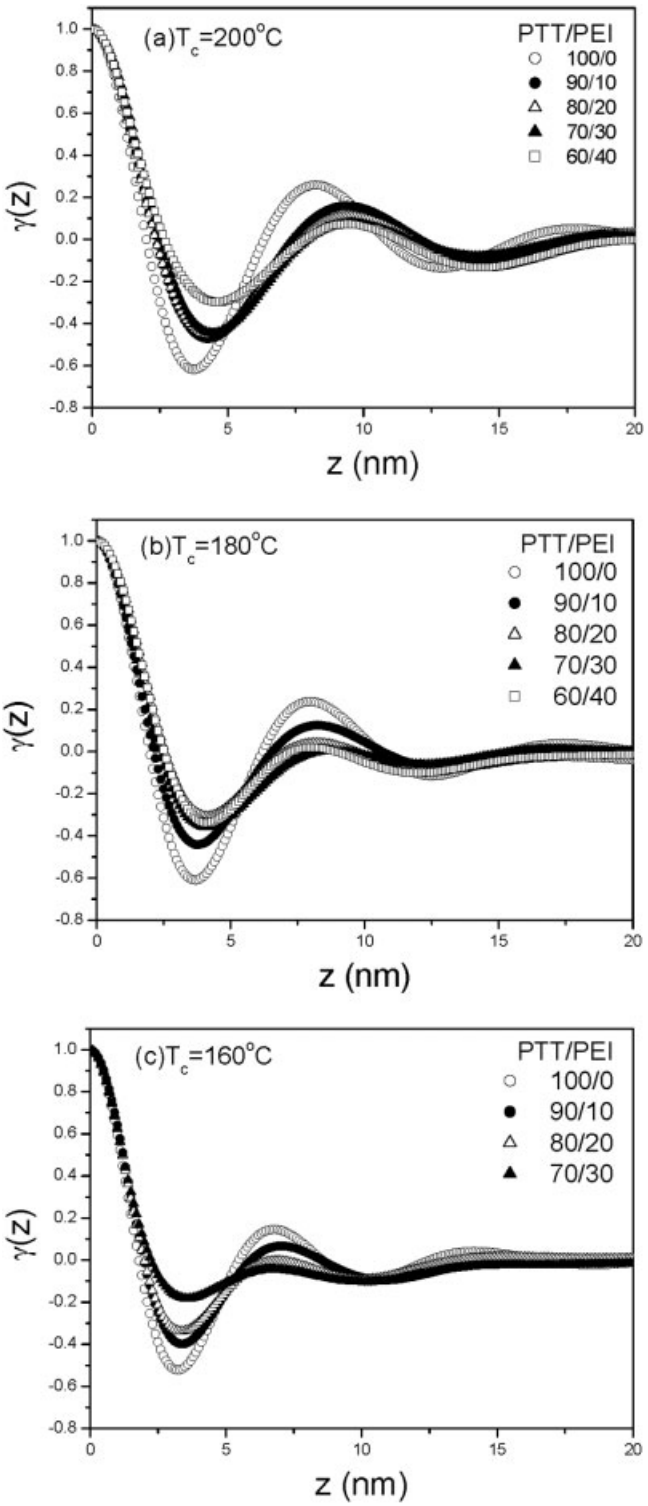

Figure 3 One-dimensional correlation functions of PTT/PEI blends crystallized at (a) T_c = 200°C; (b)T_c = 180°C; (c)T_c = 160°C.

$$l_g^* = \frac{2\sigma_e T_m^0}{\Delta h_f^0 (T_m^0 - T_c)} + \delta l \quad (7)$$

where $T_m{}^0$ is the equilibrium melting point, σ_e is the fold surface free energy, $\Delta h_f{}^0$ is the bulk enthalpy of melting per volume, and ΔT is defined as the degree of undercooling (i.e., $\Delta T = T_m{}^0 - T_c$). At low to moderate degree of undercooling, δl is small, eq. (7) thus reduces to

$$l_g^* = \frac{2\sigma T_m^0}{\Delta h_f^0 (T_m^0 - T_c)} \quad (8)$$

The final crystal thickness, according to the notation of Hoffman and Weeks,[12–13] is γ times the initial thickness, i.e.,

$$l_c = \gamma l_g^* \quad (9)$$

where γ is the so-called "lamellar thickening factor". Equation (8) prescribes that the $l_g{}^*$ is inversely proportional to the degree of undercooling. Therefore, the higher the T_c, the lower the degree of undercooling (i.e., $\Delta T = T_m{}^0 - T_c$), leading to thicken the crystal thickness. Such a consequence, the l_c value increased with elevating T_c in Figure 5(b), is attributed to the depression of undercooling.

In addition, it is worth noting in Figure 5(b) that the l_c appreciably increased for both T_c = 200 and 180°C but decreased for T_c = 160°C with the increase of PEI composition. In other words, upon blending, the crystal thickness of PTT for both T_c = 200 and 180°C increased but that for T_c = 160°C reduced. As described above, the decrease of $T_m{}^0$ would lead to the larger $l_g{}^*$ so as to form thicker crystals. The increase in

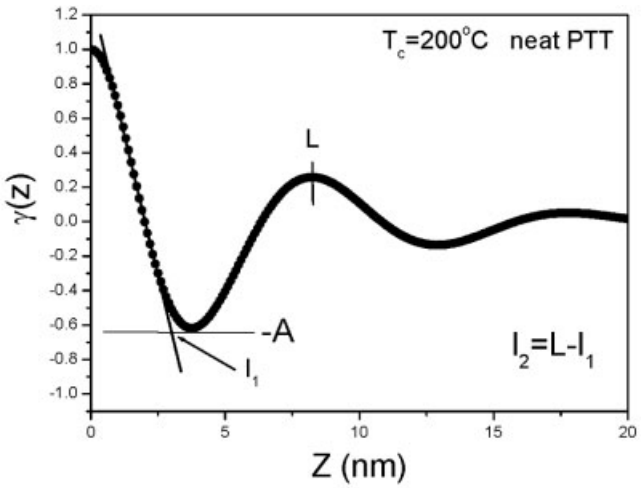

Figure 4 l_c, l_a, the most probable value of L can be estimated via simple geometric analysis of $\gamma(z)$ (the thinner length, l_1, has been assigned to be l_c and the larger length, l_2, to be l_a).

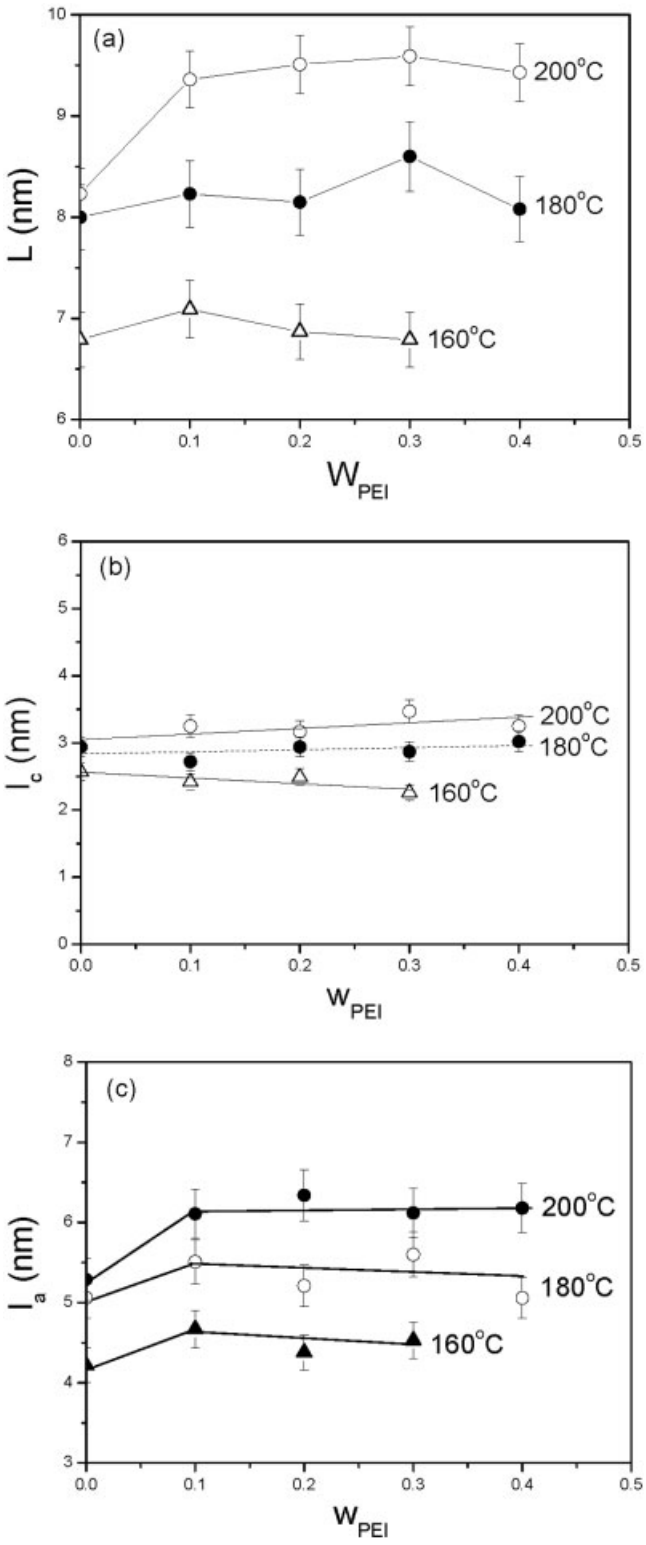

Figure 5 Variations of L, l_c, and l_a with PEI composition (a) L; (b) l_c; (c) l_a.

l_c with increasing amorphous component has been observed as reported in literature,[14–16] attributed to the depression in $T_m{}^0$ upon blending at a given T_c. Therefore, in Figure 5(b) the l_c value increased with

increasing PEI composition for T_c = 200 and 180°C, which may be ascribed to the decrease in T_m^0. Above discussion concerning the increase in l_c has mainly focused on the consideration of crystallization thermodynamics. Nevertheless, the sizes of crystals may be also affected by the crystallization kinetic factor, which may lead to the maintaining of a constant thickness of crystals even with increasing amorphous component such as i-polystyrene (iPS)/a-polystyrene (aPS),[17] sPS/aPS[18] and iPS/poly(propylene oxide) (PPO)[19] blends and so on. In Figure 5(b), the slight decrement of l_c with increasing PEI for T_c = 160°C could be also considered due to both the crystallization kinetics or morphological factors resulted.

Figure 5(c) displays the effect of PEI composition on the thickness of the amorphous layers. The trend of l_a with PEI composition for three T_cs is quite similar: l_a increased as w_{PEI} [≤] 0.1 but did not vary with further increasing PEI composition. Despite the swelling of amorphous layers, the thickness of amorphous layers was relatively independent of the PEI composition, where all blends exhibited approximately the same l_a. Because a complete interlamellar incorporation should result in a monotonic increase of amorphous layer thickness with increasing PEI composition, the observation from Figure 5(c) implies an incomplete incorporation of PEI into the interlamellar regions. In other words, some PEI molecules were expelled out of the interlamellar regions. A similar phenomenon has also been observed in PET/PEI blends.[20]

The extent of interfibrillar segregation can also be determined from the magnitude of the volume fraction of lamellar stacks (e.g., the value of ϕ_s). The magnitude of ϕ_s is closely connected with the morphological structure. In the case of complete interlamellar segregation, the whole sample is homogeneously filled with lamellar stacks, so ϕ_s = 1. A smaller ϕ_s implies a larger extent of interfibrillar segregation. Figure 6 depicts the variations of ϕ_c, ϕ_c^{lin}, and ϕ_s with PEI composition. ϕ_s remained essentially constant at approximately unity when w_{PEI} [≤] 0.1. In this case, PEI molecules were predominantly incorporated into the interlamellar regions. When $w_{PEI} > 0.1$, the ϕ_s obviously dropped with PEI composition, indicating the existence of extralamellar segregation after PTT crystallization, and the extent of extralamellar segregation increased with increasing of PEI composition.

In addition, in Figure 2(c) a strong intensity upon at the low-q region can be observed for blends of 60/40–50/50 blends crystallized at T_c = 160°C. The abrupt intensity at the low-q region is termed "zero-angle scattering." The observed scattering patterns on the 60/40–50/50 blends crystallized at T_c = 160°C are characterized by the superposition of a monotonically decayed profile and a scattering peak associated with PTT lamellar stacks. The large low-q intensity or

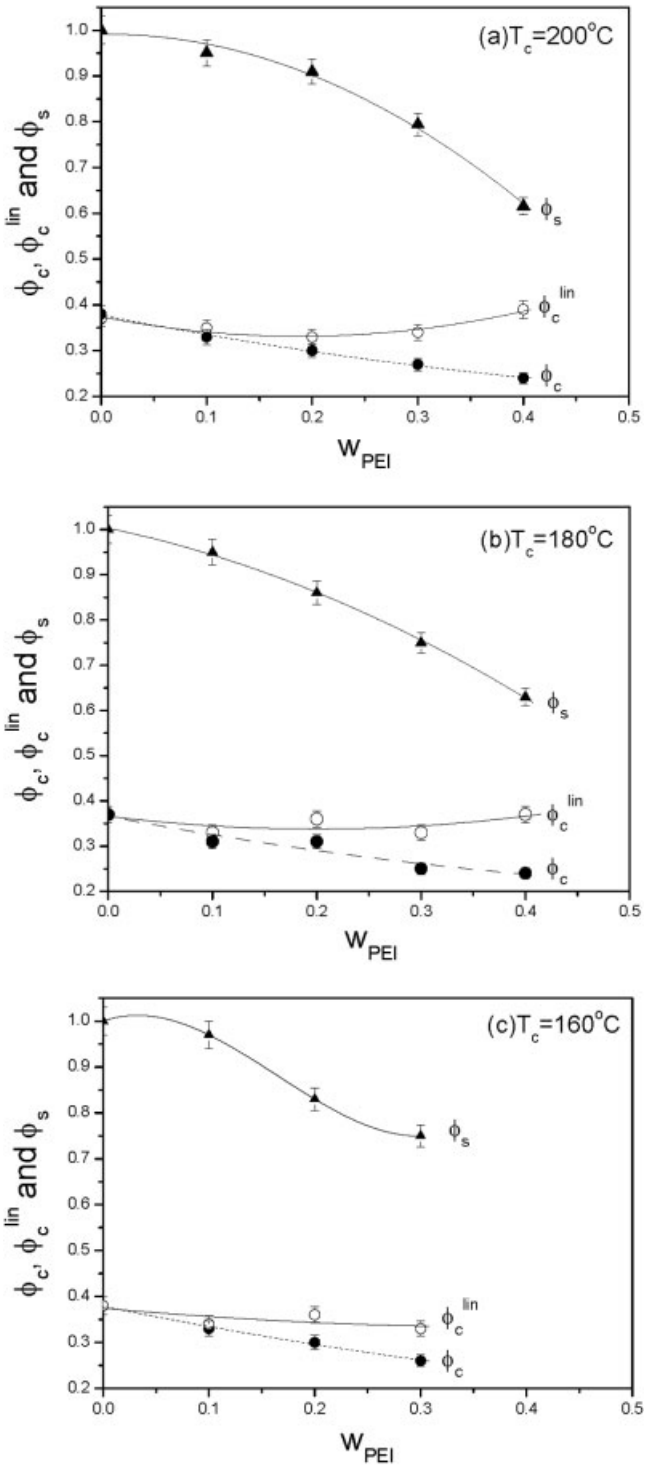

Figure 6 Variations of ϕ_c, ϕ_c^{lin} and ϕ_s with PEI composition (a) T_c = 200°C; (b)T_c = 180°C; (c)T_c = 160°C.

"zero-angle scattering" signifies the presence of heterogeneity having a size larger than the crystalline and amorphous layers. According to Schultz,[21] the zero-angle scattering may be attributed to a large (greater than lamellar length scales) individual amorphous domain inserted into the stacks of several lamellae to

create a gap in the lamellar stacks. The electron density contrast between this large amorphous domain and the stacking of alternating crystalline–amorphous layers gives rise to the zero-angle scattering. In PTT/PEI blends, the larger amorphous domains exterior to the PTT lamellar stack referred to the PEI molecules, which are located in the interfibrillar regions. These exterior amorphous domains were generated as PEI was segregated beyond several layers of lamellae. This type of zero-angle scattering has also been observed in PET/PEI blends,[20] where the morphology was induced by a combined crystallization and liquid–liquid demixing.

It should be noted that zero-angle scattering does not necessarily appear in the Lorentz-corrected profiles even if interfibrillar segregation is evident. If the interfibrillar segregation distance is so large (e.g., approaches the order of micrometers) that the amorphous diluent is expelled beyond many layers of lamellae, the interference between the resultant large lamellar stack domains and interfibrillar amorphous domains could generate the zero-angle scattering at the q region that is too small to be accessed by the typical SAXS instrument. In the present study, for the blends crystallized at T_c = 200 and 180°C, the amorphous PEI was expelled beyond many layers of PTT lamellae, the interference between the resultant large PTT lamellar stack domains and interfibrillar amorphous domains of amorphous PEI could generate the zero-angle scattering at the q region that is too small to be accessed by the typical SAXS instrument. Therefore, it may be suggested that the distance of PEI segregation at T_c = 160°C is shorter than those at T_c = 200 and 180°C.

CONCLUSIONS

The lamellar morphology of PTT/PEI blends has been investigated by means of POM and SAXS. From the observation under POM, it was suggested that PEI was predominantly segregated into the interlamellar and/or interfibrillar regions upon PTT crystallization since the PTT spherulitic morphologies of blends were volume-filling. On the basis of the composition variation of l_a, the magnitude of ϕ_s revealed that amorphous PEI was located in the interlamellar regions of PTT as w_{PEI} [≤] 0.1, while amorphous PEI was predominantly segregated into the interfibrillar regions of PTT as $w_{PEI} > 0.1$, and the extent of interfibrillar segregation increased with increasing w_{PEI}. The zero-angle scattering can be observed only for 60/40 and 50/50 blends crystallized at T_c = 160°C but not for those crystallized at T_c = 200 and 180°C from the Lorentz-corrected SAXS profiles. This may be attributed to the fact that amorphous PEI at T_c = 200 and 180°C was segregated beyond many layers of PTT lamellae, the interference between the resultant PTT large lamellar stack domains and interfibrillar amorphous domains of PEI could generate the zero-angle scattering at the q region that is too small to be accessed by the typical SAXS instrument. Therefore, it may be suggested that the distance of PEI segregation at T_c = 160°C is shorter than those at T_c = 200 and 180°C.

We are grateful for the support of SAXS beamtime from Prof. Show-An Chen at the Department of Chemical Engineering, National Tsing Hua University, Taiwan.

References

1. Brown, H. S.; Chuah, H. H. Chem Fibers Int 1997, 47, 72.
2. Chuah, H. H. Chem Fibers Int 1996, 46, 424.
3. Dangayach, K.; Chuah, H. H.; Gergen, W.; Dalton, P.; Smith, F. Plastics Saving Planet Earth, 55th ANTEC Proceedings: 1997, 2097.
4. Chuah, H. H.; Lin, V. D.; Soni, U. Polymer 2001, 42, 7137.
5. Pyda, M.; Boller, A.; Grebowicz, J; Chuah, H. H.; Lebedev, B. V.; Wunderlich, B. J Polym Sci Polym Phys Ed 1998, 36, 2499.
6. Huang, J. M.; Chang, F. C. J Appl Polym Sci 2002, 84, 850.
7. Grebowicz, J. S; French, R. N. Thermochimica Acta 2003, 396, 133.
8. Strobl, G. R.; Schneider, M. J Polym Sci Polym Phys Ed 1980, 18, 1343.
9. Debye, P.; Bueche, A. M. J Appl Phys 1949, 20, 518.
10. Ruland, W. J J Appl Crystallogr 1971, 4, 70.
11. Porod, G.; Kolloid-Z. Polym 1951, 124, 83.
12. Hoffman, J. D.; Weeks. J. J. J Res Natl Bur Stand A: Phys Chem. 1962, 66A, 13.
13. Hoffman, J. D; Miller, R. L. Polymer 1997, 38, 3351.
14. Talibuddin, S.; Wu, L.; Runt, J. P.; Lin, J. S. Macromolecules 1996, 29, 7527.
15. Chen, H. L.; Wang, S. F.; Lin, T. L. Macromolecules 1998, 31, 8924.
16. Chiu, H. J; Chen, H. L.; Lin, T. L.; Lin, J. S. Macromolecules 1999, 32, 4969.
17. Warner, F. P.; MacKnight, W. J.; Stein, R. S. J Polym Phys Ed 1977, 15, 2113.
18. Wang, C.; Liao, W. P.; Cheng, Y. W.; Lin, T. L. Polymer 2004, 45, 961.
19. Wening, W.; Karase, F. E.; MacKnight, W.J. J Appl Phys 1975, 46, 4194.
20. Chen, H. L.; Hsiao, M. S. Macromolecules 1998, 31, 6579.
21. Schultz, J. M. J Polym Sci Polym Phys Ed 1973, 14, 2291.